Heliyon 9 (2023) e16690

Contents lists available at ScienceDirect

Heliyon

journal homepage: www.cell.com/heliyon

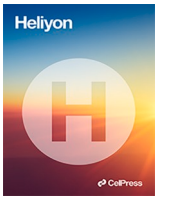

# Radiological assessment in beach sediment of coastline, Ghana

Esther Osei Akuo-ko [a], Mohammademad Adelikhah [a], Eunice Amponsem [b], Anita Csordás [a], Tibor Kovács [a,*]

[a] Institute of Radiochemistry and Radioecology, Research Centre for Biochemical, Environmental and Chemical Engineering, University of Pannonia, 8200 Veszprém, Hungary
[b] GIS Department, Wallulel Ghana Limited, Accra, Ghana

ARTICLE INFO

*Keywords:*
Radioactivity
Radiological hazard
Absorbed dose
Sediment
Interpolations
Ghana

ABSTRACT

The natural and artificial radioactivity in beach sediment sampled from the coastline of Ghana were analyzed using High Purity Germanium gamma ray detector. The overall average activity concentrations of $^{226}$Ra, $^{232}$Th, $^{40}$K and $^{137}$Cs were estimated to be 43 ± 6, 22 ± 1, 393 ± 74 and 8.4 ± 0.5 Bqkg$^{-1}$, respectively. Apart from $^{226}$Ra the mean activity concentrations of the measured radionuclides were below the world averages of 32, 45, 412 and 18.2 Bqkg$^{-1}$ respectively. High $^{137}$Cs mean concentration of 109.8 Bqkg$^{-1}$ was observed for one of the locations, which might be due to the occurrence of a nuclear incidence or other factors. The evaluated radiological parameters also had values below world averages, except for some coastal areas which recorded Annual Gonadal Dose Equivalent (AGDE) values higher than the reference level of 300 μSvy$^{-1}$. There was no significant risk associated with the radionuclide activities evaluated along the coast of Ghana. The correlation between the radionuclides and the radiological parameters were analyzed with the Pearson correlation matrix, cluster and PCA analysis, and they all showed similar outcomes. Spatial distribution maps were also created using ArcGIS software for a pictorial view of the distribution of radionuclides along the study area.

## 1. Introduction

Natural radiation has exposed the world's population to radionuclides by means of external sources such as sediment and cosmic radiation and inner radiation of the body by radionuclides [1]. Radionuclides are present in the environment as they exist in different environmental media e.g. sediment, rock, soil, sand, air and water. Their concentrations in these elements are determined by the geological formations of the area. Beach sediments are key environmental media for evaluating the health risks associated with gamma radiation exposure [2,3]. Thus, they are means of identifying the levels of radioactivity and radiation risks in the human environment since they are known to contain radionuclides. Humans receive approximately 87% of radiation doses from natural radiation sources and these originate from naturally occurring radioactive radionuclides of $^{238}$U, $^{232}$Th and their daughters and $^{40}$K [4]. Radionuclides can cause detrimental biological effects to the DNA and as well as cause cancer since they consist of essential source of ionizing radiation harmful to humans and non-humans [5,6].

Sediment has been recognized as a medium offering valuable information regarding environmental and geochemical contamination by radionuclides [1]. Sediments and soils contain radionuclides including $^{238}$U, $^{210}$Po, $^{232}$Th, $^{226}$Ra, $^{228}$Th, $^{228}$Ra, and $^{40}$K which

* Corresponding author.
*E-mail address:* kovacs.tibor@mk.uni-pannon.hu (T. Kovács).

https://doi.org/10.1016/j.heliyon.2023.e16690
Received 17 November 2022; Received in revised form 2 May 2023; Accepted 24 May 2023
Available online 25 May 2023

are extensively distributed in the environment by reason of their natural existence in the earth crust and atmosphere [5,7,8]. In general, sediments have been accepted and used as tracers and environmental indicators for radionuclide contamination sources, along with monitoring such contaminations [9]. Sediment provides the working information necessary for the assessment of the radiological hazards related to gamma radiation exposure through its activity concentrations, which helps to establish reference database to evaluate potential radiological change [3]. They behave as reservoirs of materials that are derivative from both anthropogenic and natural weathering processes [10,11]. Furthermore, sediments act as means of migration for the transference of radionuclides in the aquatic ecosystem [4]. Over the years, investigations into the evaluation of the level of radioactivity concentrations in sediments and coastal sands have been carried out all over the world [2,8–13]. The worldwide average concentration values of the radionuclides $^{226}$Ra, $^{232}$Th and $^{40}$K in sediment samples are 32, 45 and 412 Bqkg$^{-1}$, respectively. However, in some countries like Iran, Brazil and China, these values can be higher due to the high concentrations of uranium, radium and thorium in their soils [14,15].

The concern for understanding the behavior of artificial radionuclides such as $^{137}$Cs in the environment and atmosphere is as a result of the 1986 Chernobyl nuclear accident and the 1950s nuclear weapon test in the Northern and Southern Hemispheres, which led to the release of $^{137}$Cs into the atmosphere in great quantities [8,11,13]. The recent nuclear power plant accident in Fukushima in 2011 also led to the distribution of $^{137}$Cs in the atmosphere [16–18]. Since it has already been established that the marine environment aids in the transfer of radionuclides from one location to another, the coast of West Africa could be affected by the polluted areas due to ocean and atmospheric distribution despite the absence of nuclear power plants [5].

The Ghanaian coastline has considerable economic and ecological value. Activities in the coastal area include fishing, tourism, oil exploitation, energy production and import and export activities. The fast growth of the population and infrastructure expansion along the coast of the country could lead to elevated levels of radioactivity [11]. Therefore, investigations of radioactivity in the coastal environment are beneficial for the safety of human health from the deleterious effects of ionizing radiation. Some studies have been conducted in previous years to evaluate the radioactivity levels in sediment in selected coastal zones in Ghana [5,9,11]. These studies determined activity concentrations using gamma spectrometry and some radiological risks were assessed. Despite these efforts, their studies did not cover the entire coastal area of Ghana. This is particularly important as the country takes steps to select a site for its nuclear power plant in the near future [19,20] and this survey will give some baseline information on the radioactivity levels along the Ghanaian coast.

Therefore, a study of activity concentrations of radionuclides in the Ghanaian beach sediment is crucial for both human and environmental perspectives. The objective of this study is to measure the activity concentrations of natural and artificial radionuclides in shore sediment, to evaluate their radiological hazards and to create interpolation maps for visual representation of the distribution of radionuclides along the Ghanaian coast.

## 2. Materials and methods

### 2.1. Study area

Ghana has a long coastline of about 550 km, which is endowed with fishery and other living resources. Approximately 25% of the Ghanaian populace live along the coast [21,22]. The coastline is habited by individuals who survive by fishery activities and using beach sand for building purposes. Again, the coastline is a very popular site for holiday makers and tourists. For these reasons, it is significant to substantiate the magnitude of any abnormality along the coast with regards to radioactivity levels. In this study, the coastal area covered was from the geological latitude between 5°0'44.64''N 2°42'44.38''W and 6°6'21.88''N 1°11'4.02''E.

### 2.2. Sample collection and preparation

A plastic core tube of diameter 7 cm was used to collect the sediment samples. Two sites with a distance of 100–200 m from each other were selected as sub-sampling points at every coastal sampling location. In each sampling location an area of 1 m$^2$ was marked and four subsamples were collected i.e., three samples from the corners and one from the center of the marked area. The samples were collected from a depth of 25–50 cm above the ground and 100–150 m away from the seawater [8]. A total of 19 coastal areas were sampled with 152 samples collected from the coastal areas altogether. The collected sediment samples were stored in Ziploc bags, correctly labelled as at the time of sampling and sent to the environmental laboratory of the Institute of Radiochemistry and Radioecology of the University of Pannonia, Veszprem, Hungary for analysis.

In the laboratory, the organic materials such as plants, dead small animals, shells, etc. were removed from the samples, and they were air dried for at least a week. Then they were pulverized, sieved with a 3 mm sieve and oven dried at a temperature of 105 °C for 24 h. Afterwards, the subsamples for every single coastal location were homogenized to make one sample and then 595–600 g of the homogenized sample was transferred into corresponding labelled Marinelli beaker. They were well-sealed for four weeks to allow secular equilibrium to be established between the long-lived parent and daughter nuclides before being counted by the gamma spectrometry.

### 2.3. Gamma spectroscopic analysis

The activity of $^{226}$Ra, $^{232}$Th, $^{40}$K and $^{137}$Cs in the beach sediment samples were determined by using a semiconductor High Purity Germanium (HPGe) detector (ORTEC GMX40-76 with an efficiency of 40%). The APTEC multi-channel analyzer (MCA) software was used to analyze the gamma spectra generated. Three closed sources were used to calibrate the detector. These were $^{137}$Cs with a peak

energy of 662 keV, $^{60}$Co with two peak energies of 1173 and 1332 keV and $^{241}$Am with a peak energy of 59 keV. The IAEA-375 reference material having similar samples' geometry with known activity of radionuclides was used to calculate the detection efficiency of each peak [8,23–25]. Specific gamma peaks were used to calculate the activity concentration of each radionuclide: $^{137}$Cs = 661.6 keV (Pγ: 84.9%), $^{40}$K = 1460.8 keV (Pγ: 10.6%), $^{226}$Ra = using its decay products ($^{214}$Pb and $^{214}$Bi) peak energies as $^{214}$Pb = 351.9 keV (Pγ: 35.3%) and $^{214}$Bi = 609.3 keV (Pγ: 45.2%), and $^{232}$Th was calculated using its decay products in equilibrium condition ($^{228}$Ac and $^{208}$Tl) peak energies as $^{228}$Ac = 911.2 keV (Pγ: 26%), $^{208}$Tl = 583.2 and 2614.5 keV (Pγ: 30.5% and 35.8%). For the achievement of better statistics in gamma spectra and to obtain minimum counting error, each measurement was carried out with a counting time of 80,000 s [23,25,26].

### 2.4. Radiological risk assessment

The radioactivity concentration of the radionuclide in the beach sediment, minimum detectable activity (MDA) and uncertainty were evaluated in this work. Radiological parameters such as external hazard index, absorbed dose rate, radium equivalent activity and annual effective dose were determined to estimate the likely radiological hazards and radiation risks to the population.

Below is a table showing the specific peak detection efficiency and MDA of $^{226}$Ra, $^{232}$Th, $^{40}$K and $^{137}$Cs [8].

#### 2.4.1. Activity concentration

The radionuclide activities in the sediment samples were derived from the following equation:

$$A = \frac{N}{\varepsilon \text{ x } P \text{ x } m \text{ x } t} \tag{1}$$

Where $A$ is the activity concentration of the radionuclide in Bqkg$^{-1}$, $N$ is the net area under the related full energy peaks, $\mathcal{E}$ is the detection efficiency at energy E, $P$ is the abundance of the gamma line in a radionuclide, $m$ is the mass of the sample in kg and $t$ is the count time.

#### 2.4.2. Radium equivalent activity (raeq)

Radium equivalent activity ($Ra_{eq}$) of the samples were calculated using the equation below, in view of such case that 370 Bqkg$^{-1}$ of $^{226}$Ra or 259 Bqkg$^{-1}$ of $^{232}$Th or 4810 Bqkg$^{-1}$ of $^{40}$K produce similar amount of gamma dose rate [15]:

$$Ra_{eq}\ (Bqkg^{-1}) = A_{Ra} + (A_{Th} \times 1.43) + (A_K \times 0.077) \tag{2}$$

Where $A$ represents mass activity (Bqkg$^{-1}$). The maximum permissible $Ra_{eq}$ activity is equivalent to 370 Bqkg$^{-1}$ corresponds to an effective dose of 1 mSvy$^{-1}$ [15].

#### 2.4.3. External hazard index ($H_{ex}$)

The external hazard index ($H_{ex}$) was determined with the equation below, to know whether the ICRP recommended value (1 mSvy$^{-1}$) of dose equivalent was exceeded or not, i.e., 370 Bqkg$^{-1}$ of radium equivalent activity corresponds to the external hazard index limit value as 1 [27]:

$$H_{ex} = (A_{Ra} / 370) + (A_{Th} / 259) + (A_K / 4810) \leq 1 \tag{3}$$

Where $A_{Ra}$, $A_{Th}$ and $A_K$ are the activity concentrations of the radium, thorium and potassium radionuclides respectively.

#### 2.4.4. Internal hazard index ($H_{in}$)

The internal exposure of the respiratory organs to radon and its progenies are also as hazardous as the external irradiation which is measured by $H_{in}$ and expressed as [28]:

$$H_{in} = A_{Ra} / 185 + A_{Th} / 259 + A_K / 4810 \tag{4}$$

Where $A_{Ra}$, $A_{Th}$ and $A_K$ are the activity concentrations (in Bqkg$^{-1}$) of $^{226}$Ra, $^{232}$Th and $^{40}$K, respectively.

#### 2.4.5. Gamma index ($I_\gamma$)

The gamma index indicates the collective effect of the natural radionuclides ($^{226}$Ra, $^{232}$Th and $^{40}$K) and its radiological risk related to the medium. It is expressed by the following equation [12]:

$$I\gamma = A_{Ra} / 300 + A_{Th} / 200 + A_K / 4810 \tag{5}$$

Where $A_{Ra}$, $A_{Th}$ and $A_K$ are the activity concentrations of $^{226}$Ra, $^{232}$Th and $^{40}$K radionuclides in Bqkg$^{-1}$ [12].

#### 2.4.6. Gamma dose rate (D)

The absorbed gamma dose rate (D) in the air at 1 m above the ground level due to the existence of $^{226}$Ra, $^{232}$Th, $^{40}$K and $^{137}$Cs in the sediment samples at each location was calculated with the equation below:

$$D\ (nGyh^{-1}) = (A_{Ra} \times 0.462) + (A_{Th} \times 0.621) + (A_K \times 0.0417) + (A_{Cs} \times 0.03) \tag{6}$$

Where $A_{Ra}$, $A_{Th}$, $A_K$ and $A_{Cs}$ are the activity concentration of the related radionuclides in Bqkg$^{-1}$. The values 0.462, 0.621, 0.0417 and 0.03 are the dose rate per unit of $^{226}$Ra, $^{232}$Th, $^{40}$K and $^{137}$Cs respectively [12,28].

#### 2.4.7. Annual effective dose

To evaluate the annual effective dose rates (AED) to human body, a conversion factor of 0.7 SvGy$^{-1}$ and an outdoor occupancy factor of 0.2 were used for the calculations. The annual effective dose is given as:

$$\text{AED (mSvy}^{-1}) = \text{D (Gy/h) x 8760 (h/y) x 0.2} \times 0.7\ (\text{SvGy}^{-1}) \quad (7)$$

The estimated world mean annual effective dose from outdoor terrestrial gamma radiation is 70.0 μSvy$^{-1}$ [14,15,28].

#### 2.4.8. Annual gonadal dose equivalent

The annual gonadal dose equivalent (AGDE) considers the effect of radiation on living cells. Such impacts could be the mutation of organism cells or death. The UNSCEAR is particular about the effect of radiation on the active bone marrow and bone surface cells of an organism. The AGDE due to the specific activities of $^{226}$Ra, $^{232}$Th and $^{40}$K was determined with the equation:

$$\text{AGDE (μSvy}^{-1}) = (A_{Ra} \times 3.09) + 4.18\ (A_{Th} \times 4.18) + (A_K \times 0.314) \quad (8)$$

Where $A_{Ra}$, $A_{Th}$, and $A_K$ are the activity concentrations of the related radionuclides in Bqkg$^{-1}$ [12, 15].

### 2.5. Spatial distribution

In this paper, interpolation maps used to visualize the appropriate spatial distribution of a variable to its position. The ArcGIS software was used in this regard to give a clear understanding of the spatial distribution of the radionuclides along Ghana's coast. The ordinary kriging (OK) technique was applied as it's one of the most flexible and precise techniques for spatial distribution and a fundamental method in geostatistics. The technique has been identified as the best linear unbiased estimator. It produces visually smart maps and suitable in detecting a trend from unevenly spaced data. As a result, it has been used in numerous studies to evaluate the distribution of radionuclides in the environment and for creating of radiological maps [8,29].

### 2.6. Statistical analyses

The statistical analyses for this work were done using the IBM SPSS software version 26. The normal distribution of the data was tested with the Kolmogorov-Smirnov test. The SPSS was used to determine the ordinary statistics of the analysis results of $^{226}$Ra, $^{232}$Th, $^{40}$K and $^{137}$Cs. The mean, annual mean, minimum, maximum, standard deviation and geometric mean were evaluated for the data set. The Pearson correlation matrix analysis, cluster analysis and principal component analysis (PCA) were used to determine the correlation and relationships between the radionuclides measure and the evaluated radiological parameters (see Table 1).

## 3. Results and discussion

### 3.1. Activity concentrations of the measured radionuclides

The activity concentrations of $^{226}$Ra, $^{232}$Th, $^{40}$K and $^{137}$Cs from the coastline of Ghana are presented in Table 2 below.

The measured activity concentrations of $^{226}$Ra ranged between 14 ± 4 and 134 ± 7 Bqkg$^{-1}$, 8 ± 1 and 77 ± 1 Bqkg$^{-1}$ for $^{232}$Th, 207 ± 75 and 1273 ± 69 Bqkg$^{-1}$ for $^{40}$K and 1.1 ± 0.6 and 111.4 ± 0.3 Bqkg$^{-1}$ for $^{137}$Cs. The mean activity concentrations were determined to be 43 ± 6 Bqkg$^{-1}$, 22 ± 1 Bqkg$^{-1}$, 393 ± 74 Bqkg$^{-1}$ and 8.4 ± 0.5 Bqkg$^{-1}$ for $^{226}$Ra, $^{232}$Th, $^{40}$K and $^{137}$Cs, respectively. The mean $^{137}$Cs activity concentration for Dixcove (109.8 ± 0.3 Bqkg$^{-1}$) affected the overall $^{137}$Cs mean for the study. The $^{226}$Ra concentrations in the sediment samples for this study were higher than all the concentrations of $^{232}$Th. According to the results presented in Table 2, some of the sample locations had concentrations exceeding the world mean concentrations set by the UNSCEAR (2008). Activity concentrations of $^{226}$Ra for Komenda, Cape Coast, Anomabo, Bortianor, Tema, Keta and Prampram were higher than the world mean of 32 Bqkg$^{-1}$ [14]. $^{232}$Th average concentration for Keta was almost 30 Bqkg$^{-1}$ more than the world mean. Studies show that beach sediment samples are mainly mineral deposits formed from weathering and erosion of metamorphic and igneous rocks. These rocks are rich in uranium and thorium and therefore major sources of $^{226}$Ra and $^{232}$Th in sediment. Again, the decay of uranium and thorium in seawater leads to the pollution of sediment with $^{226}$Ra and $^{232}$Th, which at the end are deposited along the shore by wave action and tides [11]. Also, Sekondi, Labadi, Half Assin and Cape 3 Points had average $^{40}$K activity levels exceeding the world mean of

**Table 1**
Minimum detectable activity and specific peak detection efficiency$^{226}$Ra,$^{232}$Th,$^{40}$K and$^{137}$Cs.

| Radionuclide | Specific peak detection efficiency | MDA (Bqkg$^{-1}$) |
|---|---|---|
| $^{226}$Ra | 2.40% | 0.5 |
| $^{232}$Th | 1.40% | 0.7 |
| $^{40}$K | 1.20% | 23 |
| $^{137}$Cs | 2.20% | 0.5 |

**Table 2**
Activity concentration of radionuclides measured in beach sediment from the Ghanaian coastline.

| Locations | $^{226}$Ra (Bqkg$^{-1}$) | | | $^{232}$Th (Bqkg$^{-1}$) | | | $^{40}$K (Bqkg$^{-1}$) | | | $^{137}$Cs (Bqkg$^{-1}$) | | |
|---|---|---|---|---|---|---|---|---|---|---|---|---|
| | Subsample I | Subsample II | Mean | Subsample I | Subsample II | Mean | Subsample I | Subsample II | Mean | Subsample I | Subsample II | Mean |
| 1. Axim | 19 ± 5 | 17 ± 5 | 18 ± 5 | 13 ± 2 | 11 ± 2 | 12 ± 2 | 287 ± 77 | 282 ± 77 | 285 ± 77 | 1.8 ± 0.5 | 1.4 ± 0.5 | 1.6 ± 0.5 |
| 2. Dixcove | 15 ± 4 | 19 ± 4 | 17 ± 4 | 9 ± 1 | 14 ± 1 | 12 ± 1 | 284 ± 75 | 280 ± 75 | 282 ± 75 | 108.2 ± 0.3 | 111.4 ± 0.3 | 109.8 ± 0.3 |
| 3. Takoradi | 23 ± 5 | 23 ± 5 | 23 ± 5 | 9 ± 1 | 8 ± 1 | 9 ± 1 | 319 ± 74 | 325 ± 74 | 322 ± 74 | 2.1 ± 0.7 | 1.3 ± 0.7 | 1.7 ± 0.7 |
| 4. Sekondi | 27 ± 6 | 33 ± 6 | 30 ± 6 | 13 ± 1 | 10 ± 1 | 12 ± 1 | 1267 ± 69 | 1273 ± 69 | 1270 ± 69 | 2.2 ± 0.3 | 2.4 ± 0.3 | 2.3 ± 0.3 |
| 5. Komenda | 51 ± 6 | 45 ± 6 | 48 ± 6 | 10 ± 1 | 9 ± 1 | 10 ± 1 | 335 ± 73 | 338 ± 73 | 337 ± 73 | 2.7 ± 0.7 | 1.9 ± 0.7 | 2.3 ± 0.7 |
| 6. Cape Coast | 39 ± 5 | 37 ± 5 | 38 ± 5 | 15 ± 1 | 19 ± 1 | 17 ± 1 | 253 ± 74 | 252 ± 74 | 253 ± 74 | 3.4 ± 0.4 | 3.8 ± 0.4 | 3.6 ± 0.4 |
| 7. Anomabo | 72 ± 6 | 79 ± 6 | 75 ± 6 | 26 ± 1 | 24 ± 1 | 25 ± 1 | 382 ± 73 | 378 ± 73 | 380 ± 73 | 4.1 ± 0.5 | 4.2 ± 0.5 | 4.2 ± 0.5 |
| 8. Saltpond | 23 ± 6 | 21 ± 6 | 22 ± 6 | 14 ± 1 | 11 ± 1 | 13 ± 1 | 378 ± 73 | 377 ± 73 | 378 ± 73 | 1.1 ± 0.6 | 1.2 ± 0.6 | 1.2 ± 0.6 |
| 9. Winneba | 31 ± 6 | 39 ± 6 | 35 ± 6 | 12 ± 1 | 13 ± 1 | 13 ± 1 | 273 ± 75 | 280 ± 75 | 277 ± 75 | 2.7 ± 0.7 | 3.2 ± 0.7 | 3.0 ± 0.7 |
| 10. Bortianor | 128 ± 5 | 133 ± 5 | 130 ± 5 | 61 ± 1 | 58 ± 1 | 59 ± 1 | 312 ± 74 | 302 ± 74 | 307 ± 74 | 2.8 ± 0.7 | 2.3 ± 0.7 | 2.6 ± 0.2 |
| 11. Labadi | 27 ± 6 | 26 ± 6 | 27 ± 6 | 14 ± 1 | 16 ± 1 | 15 ± 1 | 549 ± 72 | 543 ± 72 | 546 ± 72 | 2.4 ± 0.6 | 1.9 ± 0.6 | 2.2 ± 0.6 |
| 12. Tema | 65 ± 5 | 67 ± 5 | 66 ± 5 | 33 ± 1 | 34 ± 1 | 34 ± 1 | 207 ± 75 | 214 ± 75 | 211 ± 75 | 2.1 ± 0.5 | 2.3 ± 0.5 | 2.2 ± 0.5 |
| 13. Ada Foah | 26 ± 7 | 19 ± 7 | 23 ± 7 | 10 ± 1 | 9 ± 1 | 9 ± 1 | 311 ± 75 | 314 ± 75 | 313 ± 75 | 3.1 ± 0.7 | 2.5 ± 0.7 | 2.8 ± 0.7 |
| 14. Keta | 131 ± 7 | 134 ± 7 | 133 ± 7 | 77 ± 1 | 74 ± 1 | 76 ± 1 | 358 ± 73 | 352 ± 73 | 355 ± 73 | 2.4 ± 0.5 | 3.1 ± 0.5 | 2.8 ± 0.5 |
| 15. Half Assin | 23 ± 6 | 20 ± 6 | 22 ± 6 | 23 ± 2 | 26 ± 2 | 25 ± 2 | 426 ± 77 | 430 ± 77 | 428 ± 77 | 2.0 ± 0.5 | 2.5 ± 0.5 | 2.3 ± 0.5 |
| 16. Jomoro | 30 ± 7 | 31 ± 7 | 31 ± 7 | 27 ± 2 | 28 ± 1 | 27 ± 2 | 294 ± 77 | 302 ± 77 | 298 ± 77 | 2.6 ± 0.6 | 2.2 ± 0.6 | 2.4 ± 0.6 |
| 17. Cape 3 Points | 17 ± 4 | 16 ± 4 | 16 ± 4 | 12 ± 1 | 14 ± 1 | 13 ± 1 | 560 ± 76 | 567 ± 76 | 564 ± 76 | 7.1 ± 0.6 | 7.8 ± 0.6 | 7.5 ± 0.6 |
| 18. Prampram | 49 ± 6 | 44 ± 6 | 47 ± 6 | 30 ± 2 | 33 ± 2 | 31 ± 2 | 361 ± 76 | 354 ± 76 | 357 ± 76 | 4.3 ± 0.5 | 3.5 ± 0.5 | 3.9 ± 0.5 |
| 19. Aflao | 14 ± 4 | 15 ± 4 | 15 ± 4 | 9 ± 1 | 10 ± 1 | 9 ± 2 | 301 ± 76 | 307 ± 76 | 304 ± 76 | 1.7 ± 0.6 | 1.8 ± 0.6 | 1.8 ± 0.6 |
| Current study (mean) | **43 ± 6** | | | **22 ± 1** | | | **393 ± 74** | | | **8.4 ± 0.5** | | |
| World mean [14] | **32** | | | **45** | | | **412** | | | **18.2** | | |
| Geometric mean | 34 | | | 18 | | | 358 | | | 3.1 | | |
| Median | 30 | | | 13 | | | 322 | | | 2.4 | | |
| Minimum | 14 | | | 8 | | | 207 | | | 1.1 | | |
| Maximum | 134 | | | 77 | | | 1273 | | | 111.4 | | |
| Standard deviation | 35 | | | 18 | | | 230 | | | 24.6 | | |
| Skewness | 2 | | | 2 | | | 3 | | | 4.3 | | |
| Kurtosis | 3 | | | 4 | | | 13 | | | 18.9 | | |

412 Bqkg$^{-1}$ with the highest being 1270 ± 69 Bqkg$^{-1}$ observed at Sekondi [14]. This coastal location is about 100 m away from a hilly land area with a vast green vegetation and agricultural activities in some parts of the land particularly the cultivation of plantain crops. This could contribute to the concentration of $^{40}$K in sediment through leaching. Again, the use of artificial fertilizers on the crops which might have leached down through the soils to sediments along the coast [2] could result in the 1270 ± 69 Bqkg$^{-1}$ activity concentration observed at this coastal area.

In the case of artificial radionuclide in sediment along the Ghanaian coast, Dixcove recorded the highest mean activity concentration of $^{137}$Cs at 109.8 ± 0.3 Bqkg$^{-1}$ which is six times the world mean. However, earlier studies by Nyarko et al. (2011) recorded $^{137}$Cs activities below 0.4 Bqkg$^{-1}$ [11]. The high $^{137}$Cs activity resulted in the relative high overall mean value of 8.4 ± 0.5 Bqkg$^{-1}$. If the $^{137}$Cs at Dixcove is considered as an outlier, then a value of 2.7 ± 0.5 Bqkg$^{-1}$ will be the mean activity concentration of the radionuclide along the coast of Ghana. The radioactivity of $^{137}$Cs in the environment maybe due to sources such as nuclear power plants accidents, nuclear weapon tests and bomb tests [8,11,12,30]. The nuclear accidents are primarily attributed to the Chernobyl (1986) and Fukushima Daiichi (2011) accidents where large quantities of $^{137}$Cs of about 85 PBq and 12 PBq, respectively were dispersed into the global atmosphere. A significant fraction of them were deposited into the sea and in coastal sediment [16,31]. Thus, existence of $^{137}$Cs in sediment at Dixcove could be as a result of the recent nuclear accident in Fukushima considering the 30.2 years half-life of $^{137}$Cs. Also, during the bomb tests large portions of the bomb-derived $^{137}$Cs were released into the stratosphere and distributed all over the earth before slowly falling to the surface of the earth primarily by precipitation [16,32]. Studies has also shown that $^{137}$Cs has a strong retention ability on the surface of different soils, owing to the presence of organic matter and clay minerals in the soils. This means it is likely that the organic matter composition in the sediment from Dixcove could have affected the retention and migration of the $^{137}$Cs radionuclide through the modification of the adsorption properties of the clay minerals in the sediment. Thus, due to this phenomenon $^{137}$Cs gets trapped in sediment restricting its movement [32–36]. Again, high $^{137}$Cs activity concentration is known to be influenced by fine-grain particles as the concentration increases with decreasing particle sizes [17,18,31]. Hence the $^{137}$Cs levels detected at Dixcove could be as a result of any of the above circumstances or a combination of them. Therefore, it would be necessary for further investigations and monitoring of $^{137}$Cs activity concentration particularly at Dixcove since this radionuclide is not naturally found in the environment but rather as a result of fallouts of nuclear power accidents and nuclear weapon tests.

The activity concentrations of the radionuclides measured in the current study were compared to previous studies conducted along the coast of Ghana. For example, Amekudzie et al., (2011) examined natural radioactivity levels along the coast of Greater Accra [9]. A comparison of their data for Labadi to the current study, $^{232}$Th was higher in concentration (732.6 Bqkg$^{-1}$) than it was observed for this study (15 ± 1 Bqkg$^{-1}$). Likewise, for $^{226}$Ra which was 140.8 Bqkg$^{-1}$ as opposed to 27 ± 6 Bqkg$^{-1}$ currently. Contrariwise, $^{40}$K was 43.9 Bqkg$^{-1}$, lower than the 546 ± 72 Bqkg$^{-1}$ evaluated in this study. Nyarko et al. (2011) measured $^{226}$Ra at Half Assin, Dixcove and Winneba and found the activities to be 3.5 Bqkg$^{-1}$, 1.6 Bqkg$^{-1}$ and 4.5 Bqkg$^{-1}$, respectively. The measured $^{137}$Cs for those locations were all less than 0.4 Bqkg$^{-1}$ [11]. These are below those determined in this study. Also, Botwe et al. in 2017 determined both natural and artificial radionuclide concentrations ($^{226}$Ra, $^{232}$Th, $^{40}$K and $^{137}$Cs) in Tema. Apart from $^{40}$K, which was 320 Bqkg$^{-1}$, the others had concentrations below those observed for this study [5].

Similarly, the outcomes of this study have been compared to those obtained in other locations of the world and shown in Table 3.

From Table 3, the activity concentrations of $^{226}$Ra, $^{232}$Th, $^{40}$K and $^{137}$Cs in this study were almost comparable to those measured in other locations except for Isinkaye and Emelue (2015) and SureshGandhi et al. (2014) who recorded very high levels of $^{40}$K and $^{232}$Th, respectively [4,38]. The difference in activities of the natural and artificial radionuclides from each location depends on the soil, rock and sediment compositions. Besides the high $^{137}$Cs activity recorded for Dixcove which affected the overall mean of that radionuclide for the study, the $^{137}$Cs data was also in one way or another similar to those observed in other locations of the world except for Dizman et al. (2016), who recorded very high $^{137}$Cs activity concentration [13].

### 3.2. Radiological risk assessment

In order to assess the radiological hazard of the beach sediment along the coast of Ghana, the radium equivalent ($Ra_{eq}$), external hazard index ($H_{ex}$), internal hazard index ($H_{in}$), gamma dose rate (D), gamma index ($I_\gamma$), annual effective dose (AED) and annual

**Table 3**
Comparison between mean activity concentration of radionuclides along the coast of Ghana and those reported in other parts of the world.

| Location | $^{226}$Ra (Bqkg$^{-1}$) | $^{232}$Th (Bqkg$^{-1}$) | $^{40}$K (Bqkg$^{-1}$) | $^{137}$Cs (Bqkg$^{-1}$) | Reference |
|---|---|---|---|---|---|
| Coastline of Ghana | 43 | 22 | 393 | 8.4 | Current study |
| Tema, Ghana | 14 | 30 | 325 | 1.5 | [5] |
| Argean coast, Greece | 15 | 25 | 565 | 1.3 | [8] |
| Mediterranean coast, Turkey | 12.2 | 9 | 157.7 | – | [28] |
| Bolu, Turkey | 18.2 | 17.3 | 258.3 | – | [12] |
| Rize, Turkey | 85.8 | 51.1 | 771.6 | 236.4 | [13] |
| Xiamen Island, China | 14.6 | 10.9 | 396.4 | – | [2] |
| Ordu, Giresun and Trabzon, Turkey | 20.3 | 10.8 | 502.9 | 6.1 | [29] |
| Rea Sea region, Egypt | 23.8 | 19.6 | 374.9 | – | [1] |
| Guangxi, China | 6.9 | 9.6 | 39.6 | – | [37] |
| Tamilnadu, India | 35.1 | 713.6 | 349.6 | – | [38] |
| Oguta, Nigeria | 47.9 | 55.4 | 1023 | – | [4] |
| Antalya, Turkey | 31.6 | 26.7 | 350.4 | – | [39] |

gonadal dose equivalent (AGDE) were calculated and presented in Table 4.

The $Ra_{eq}$ activity is an index that shows the specific activities of $^{226}Ra$, $^{232}Th$ and $^{40}K$ by a distinct quantity which takes into account the radiation risks related with them (see Table 5). $Ra_{eq}$ values evaluated in sediment samples had a mean of 104.7 $Bqkg^{-1}$ which is lower than the world mean of 370 $Bqkg^{-1}$ [14]. $Ra_{eq}$ is associated with the internal and external gamma doses due to radon and its progenies and since sediment are used as building materials by coastal dwellers in Ghana the maximum $Ra_{eq}$ value must not exceed 370 $Bqkg^{-1}$ [9,40,41].

The external and internal hazard indices are derived from the $Ra_{eq}$. To evaluate the suitability of sediment for building construction purposes and to assess the dose conveyed to inhabitants in a house constructed with sediment, a dose standard such as $H_{ex}$ was determined. Similarly, the hazard posed by radon and its progenies to the respiratory system, particularly the lungs, were determined by the $H_{in}$ index. As recommended by the UNSCEAR, the $H_{ex}$ and $H_{in}$ should be less than 1 to make the radiation exposure insignificant [14,15]. For this study, the calculated $H_{ex}$ index ranged between 0.1 and 0.7 with a mean of 0.3 whereas the $H_{in}$ were between 0.2 and 1.1 and had a mean of 0.4. Since sediments as building materials are known to composed of radioactive elements and capable to enhancing indoor radon accumulation in buildings [41], it was important to evaluate the radiation risk due to this exposure. From Table 4 both indices had averages less than recommended maximum of 1, that means it could be assumed that sediments from the shores of Ghana could be used as building material and does not pose elevated levels of radiation exposure.

The gamma index ($I_\gamma$) calculated with the activities of $^{226}Ra$, $^{232}Th$ and $^{40}K$ for the sampled locations are presented in Table 4. They ranged between 0.2 and 0.9 with a mean of 0.4 which is lower than the world average of 1 [5]. Thus, the collective effect of the natural radionuclides is low. The gamma absorbed dose rate (D) in air at 1 m above the ground level due to the existence of $^{226}Ra$, $^{232}Th$, $^{40}K$ and $^{137}Cs$ in the sediment samples were calculated and found to vary between 25.6 $nGyh^{-1}$ and 123.5 $nGyh^{-1}$ with an average of 50.1 $nGyh^{-1}$ lower than the world average of 60.0 $nGyh^{-1}$ [14]. The highest D value (123.5 $nGyh^{-1}$) is due to the presence of high activities of $^{226}Ra$ and $^{232}Th$ which was observed at Keta. This may be due to significant difference in the sediment characteristics such as porosity, density and humidity in this location as compared to the others.

The AED equivalent to the population due to the natural and artificial radioactivity in sediment samples were determined to vary from 31.4 $\mu Svy^{-1}$ to 151.5 $\mu Svy^{-1}$. The average value of AED was realized to be 61.5 $\mu Svy^{-1}$ lesser than the world average of 70.0 $\mu Svy^{-1}$ [14]. This indicates that to a large extent Ghanaian beaches are safe with normal background radiation and the level of public exposure to radiation is low. The AGDE is the assessment of the genetic implication of the annual radiation dose on living cells, particularly the effect on active bone marrow and bone surface cells of an organism [4,15]. The calculated AGDE levels due to the activities of the measured natural radionuclides were found between 181.6 $\mu Svy^{-1}$ and 839.9 $\mu Svy^{-1}$. Some of the coastal areas recorded AGDE values higher the world reference level of 300 $\mu Svy^{-1}$. This means radiation dose rates from such sediments may pose a health risk to humans. The radiological hazard indices examined showed that the values for the various parameters for Keta and Bortianor were affected by the high $^{226}Ra$ and $^{232}Th$ activity concentrations measured.

### 3.3. Multivariate statistical analysis

The multivariate statistical processes used for the data handling were executed using the commercial statistical software package of IBM SPSS version 26. Basic statistics, Pearson correlation, cluster analysis and principal component analysis (PCA) were performed using this software (see Fig. 1).

**Table 4**
Radiological hazard indices determined from the sampled beach sediment.

| Locations | $Ra_{(eq)}$ | $H_{ex}$ | $H_{in}$ | $I_\gamma$ | D | AED | AGDE |
|---|---|---|---|---|---|---|---|
| 1. Axim | 57.1 | 0.2 | 0.2 | 0.2 | 27.7 | 34.0 | 195.2 |
| 2. Dixcove | 54.7 | 0.1 | 0.2 | 0.2 | 29.8 | 36.6 | 187.7 |
| 3. Takoradi | 59.7 | 0.2 | 0.2 | 0.2 | 29.3 | 35.9 | 207.0 |
| 4. Sekondi | 145.3 | 0.4 | 0.5 | 0.6 | 74.5 | 91.4 | 542.7 |
| 5. Komenda | 88.3 | 0.2 | 0.4 | 0.3 | 42.5 | 52.2 | 296.1 |
| 6. Cape Coast | 81.1 | 0.2 | 0.3 | 0.3 | 38.5 | 47.2 | 265.8 |
| 7. Anomabo | 140.4 | 0.4 | 0.6 | 0.5 | 66.3 | 81.3 | 456.7 |
| 8. Saltpond | 69.2 | 0.2 | 0.2 | 0.3 | 33.8 | 41.5 | 239.5 |
| 9. Winneba | 74.6 | 0.2 | 0.3 | 0.3 | 35.8 | 43.8 | 248.6 |
| 10. Bortianor | 238.2 | 0.6 | 1.0 | 0.8 | 109.6 | 134.5 | 745.1 |
| 11. Labadi | 89.6 | 0.2 | 0.3 | 0.3 | 44.2 | 54.2 | 315.0 |
| 12. Tema | 129.8 | 0.4 | 0.5 | 0.5 | 60.0 | 73.6 | 409.1 |
| 13. Ada Foah | 59.8 | 0.2 | 0.2 | 0.2 | 29.3 | 35.9 | 206.5 |
| 14. Keta | 268.9 | 0.7 | 1.1 | 0.9 | 123.5 | 151.5 | 839.9 |
| 15. Half Assin | 90.7 | 0.2 | 0.3 | 0.3 | 43.6 | 53.4 | 306.6 |
| 16. Jomoro | 93.1 | 0.3 | 0.3 | 0.3 | 43.8 | 53.8 | 303.9 |
| 17. Cape 3 Points | 78.1 | 0.2 | 0.3 | 0.3 | 39.2 | 48.1 | 281.1 |
| 18. Prampram | 118.6 | 0.3 | 0.4 | 0.4 | 55.9 | 68.5 | 386.2 |
| 19. Aflao | 52.0 | 0.1 | 0.2 | 0.2 | 25.6 | 31.4 | 181.6 |
| Current study (mean) | **104.7** | **0.3** | **0.4** | **0.4** | **50.1** | **61.5** | **348.1** |
| World mean | **370**[a] | **≤1**[a] | **≤1**[b] | **≤1**[b] | **60**[a] | **70**[a] | 300[b] |

a = [14], b = [15].

**Table 5**
Pearson correlation matrix for the determined parameters.

| Parameters | $^{226}$Ra | $^{232}$Th | $^{40}$K | $^{137}$Cs | $Ra_{eq}$ | $H_{ex}$ | $H_{in}$ | $I_\gamma$ | D | AED | AGDE |
|---|---|---|---|---|---|---|---|---|---|---|---|
| $^{226}$Ra | 1 | | | | | | | | | | |
| $^{232}$Th | 0.92 | 1 | | | | | | | | | |
| $^{40}$K | −0.14 | −0.15 | 1 | | | | | | | | |
| $^{137}$Cs | −0.18 | −0.14 | −0.11 | 1 | | | | | | | |
| $Ra_{eq}$ | 0.94 | 0.92 | 0.15 | −0.20 | 1 | | | | | | |
| $H_{ex}$ | 0.94 | 0.92 | 0.15 | −0.20 | 1 | 1 | | | | | |
| $H_{in}$ | 0.98 | 0.94 | 0.04 | −0.19 | 0.99 | 0.99 | 1 | | | | |
| $I_\gamma$ | 0.92 | 0.91 | 0.23 | −0.20 | 0.99 | 0.99 | 0.98 | 1 | | | |
| D | 0.93 | 0.91 | 0.20 | −0.18 | 0.99 | 0.99 | 0.98 | 0.99 | 1 | | |
| AED | 0.93 | 0.91 | 0.20 | −0.18 | 0.99 | 0.99 | 0.98 | 0.99 | 1 | 1 | |
| AGDE | 0.91 | 0.89 | 0.25 | −0.21 | 0.99 | 0.99 | 0.98 | 0.99 | 0.99 | 0.99 | 1 |

### 3.3.1. Normality tests

The data were tested for normality using the Kolmogorov-Smirnov normality test. The activity levels of $^{226}$Ra and $^{232}$Th showed a normal distribution of data with *p*-values of 0.06 and 0.05, respectively. On the other side, $^{40}$K and $^{137}$Cs had *p*-values less than 0.05 hence rejecting the null hypothesis of a normal distribution of data. The data for the radionuclides were normalized by taking their natural logarithms and later plotted. Table 2 shows the statistics for the acquired data corresponding to the activities of $^{226}$Ra, $^{232}$Th, $^{40}$K and $^{137}$Cs in the sediment samples and some statistical analyses. Figs. 2–5 show the lognormal distribution of the activity concentration of the determined radionuclides.

From Table 2, the values of skewness point toward an asymmetric distribution of all the determined radionuclides as they were above zero. The kurtosis coefficient values also indicate the activity distribution of the radionuclides were not normal and asymmetric since they are above 1, hence rejecting the null hypothesis. The lack of a normal distribution of the dataset could related to the different type and source of rocks and sediment found at the different sampled locations and the complexity of minerals in the sediment samples [8,11].

### 3.3.2. Pearson correlation

The Pearson correlation analysis was used to estimate the extent of the relationship and strength of association among the factors, specifically the effect of sediment radiological factors on natural radionuclides' distribution [38]. The table below shows the result of the Pearson correlation analysis.

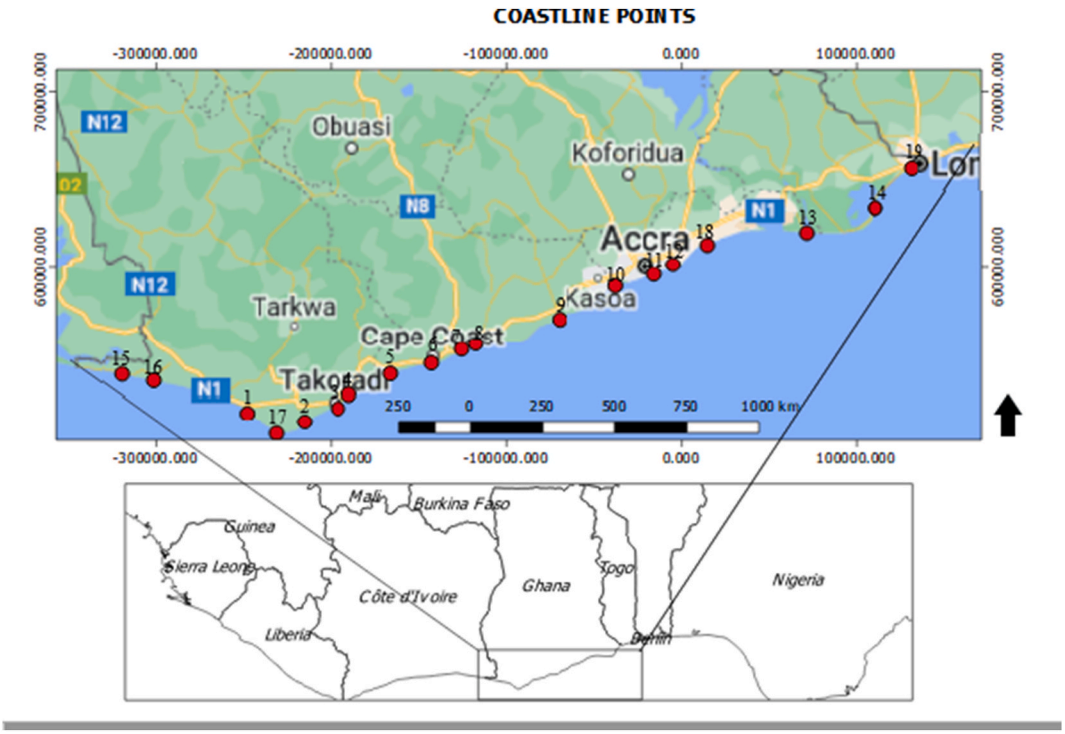


**Fig. 1.** Map of the study area and location of sampling sites.

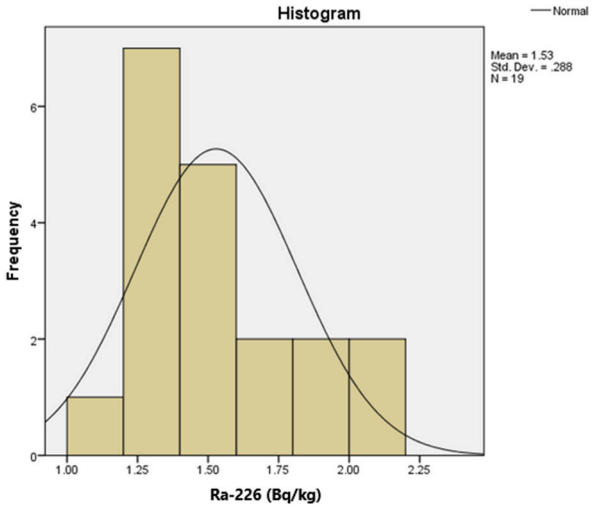


**Fig. 2.** The lognormal distribution of the activity concentration of $^{226}$Ra in Bqkg$^{-1}$..

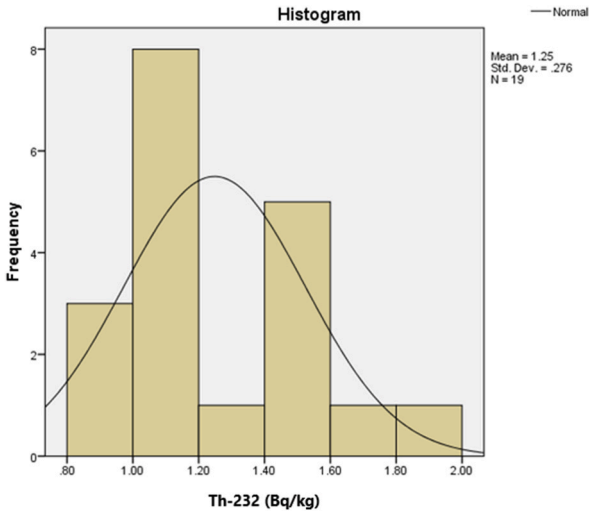


**Fig. 3.** The lognormal distribution of the activity concentration of $^{232}$Th in Bqkg$^{-1}$..

The results of the correlation show a good positive correlation coefficient ($R^2 = 0.92$) between $^{226}$Ra and $^{232}$Th, representing a strong relationship between the two radionuclides and their daughter isotopes whose decay occur together in nature [8,38]. Also, strong correlations were observed between $^{226}$Ra and $^{232}$Th and all their related radiological risk parameters ($Ra_{eq}$, $H_{ex}$, $H_{in}$, D, $I_\gamma$, AED and AGDE) since they are associated to them. However, there were weak negative correlations between $^{40}$K and $^{226}$Ra and $^{232}$Th ($R^2 = -0.14$ and $R^2 = -0.15$) which are from different decay series [8].

### 3.3.3. *Cluster analysis*

The cluster analysis was used to graphically describe the extent of relationship among the variables. The single linkage or nearest neighbor method together with correlation coefficient distance between variables were used for the cluster analysis. The single linkage cluster assumes that the similarity of two clusters is the similarity of their most similar members. This means, single linkage cluster categorizes data into clusters so that they are similar as possible within each cluster and as dissimilar as possible between clusters [38, 42]. Fig. 6 shows the results of the cluster analysis. The radiological parameters were categorized into 3 main clusters after the analysis. The first cluster showed the correlation distance of similarity between $^{226}$Ra and $^{232}$Th and the variables $Ra_{eq}$, $H_{ex}$, $H_{in}$, D, $I_\gamma$, AED and AGDE. The second cluster is associated with $^{40}$K and $^{137}$Cs with the third cluster. The composition of the first cluster shows that $^{226}$Ra and $^{232}$Th mainly influenced the radiological parameters and well correlated with them. $^{40}$K and $^{137}$Cs were in different clusters because $^{40}$K is of a different series though of natural origin and $^{137}$Cs of anthropogenic source. The results of the cluster analysis agreed with the Pearson correlation coefficient analysis.

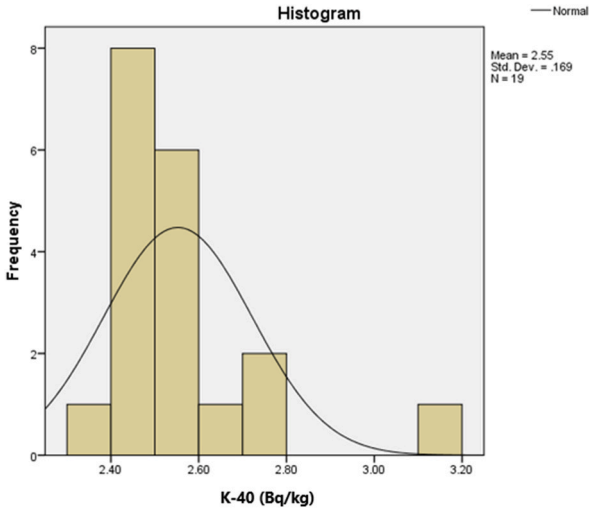


**Fig. 4.** The lognormal distribution of the activity concentration of $^{40}$K in Bqkg$^{-1}$..

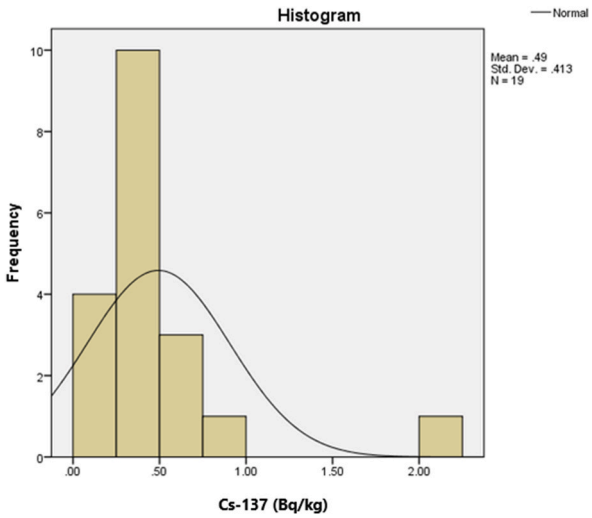


**Fig. 5.** The lognormal distribution of the activity concentration of $^{137}$Cs in Bqkg$^{-1}$..

### 3.3.4. *Principal component analysis (PCA)*

The PCA defines patterns in parameters and exhibits the data in a manner to give emphasis to similarities and differences. In this analysis, the Kaiser normalization method together with the Varimax rotation were used to develop the PCA among the variables. Eigenvalues greater than 1 criterion was used for the analysis. The eigenvalues and eigenvectors were generated from the obtained correlation matrix to determine the number of significant factors and the percent of variance explained, and they are presented in Table 6. The PCA results showed that two factors had eigenvalues greater than 1 and these two explained 90.63% of the total variance. Thus, two components were extracted from the PCA. The first component accounted for 79.88% of the rotation whereas the second accounted for 10.75%.

Fig. 7 represents the rotated factor loadings of the two components. Component 1 was categorized by a heavy loading on $^{226}$Ra, $^{232}$Th, $Ra_{eq}$, $H_{ex}$, $H_{in}$, D, $I_{\gamma}$, AED and AGDE demonstrating that $^{226}$Ra and $^{232}$Th are the main contributors of radioactivity levels in the sampled sediments. Component 2 correlated with $^{40}$K and $^{137}$Cs, showing that they are of different sources and also $^{137}$Cs is completely unrelated to the other variables as it recorded the lowest communality value of 0.147. Therefore, the results of the PCA strongly agrees with the outcomes of the Pearson correlation and cluster analyses.

## 3.4. *Spatial distribution*

Spatial distribution maps were created for the study area for a pictorial view of the distribution of radionuclides and radiological hazards along the coast of Ghana. The ordinary kriging technique was employed for the interpolation using the ArcGIS software

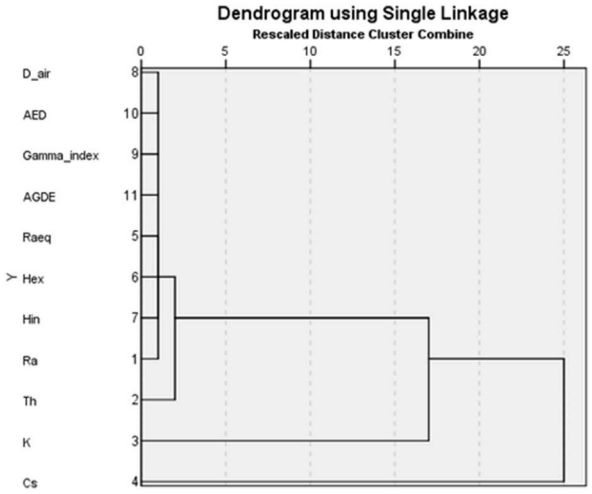


**Fig. 6.** Dendrogram of the cluster analysis between the measured radionuclides and radiological parameters.

**Table 6**
Varimax of rotated component matrix.

| Variables | Component | |
|---|---|---|
| | 1 | 2 |
| $^{226}Ra$ | 0.982 | – |
| $^{232}Th$ | 0.964 | – |
| $^{40}K$ | – | 0.971 |
| $^{137}Cs$ | −0.167 | −0.346 |
| $Ra_{eq}$ | 0.978 | 0.204 |
| $H_{ex}$ | 0.978 | 0.205 |
| $H_{in}$ | 0.993 | – |
| D_air | 0.965 | 0.252 |
| I_index | 0.960 | 0.274 |
| AED | 0.965 | 0.252 |
| AGDE | 0.952 | 0.299 |
| Variance explained (%) | **79.88** | **10.75** |

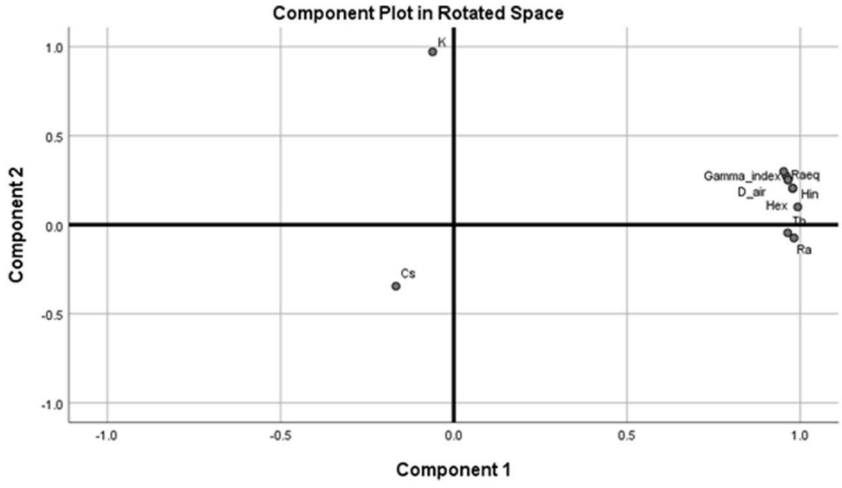


**Fig. 7.** The rotated factor loadings of the measured radionuclides and radiological parameters.

version 10.4.1. The radiological maps created used a prediction of 2.5 km from the shore to the sea to define the distribution of radionuclides for the sea, and it was protracted by 2.5 km inland to determine the distribution of radionuclides in such areas by reason of the fact that sediment is impacted by dust and particles conveyed by wind and other natural phenomenon [29]. Fig. 8 represents the interpolation maps for $^{226}$Ra, $^{232}$Th, $^{40}$K, $^{137}$Cs, $Ra_{eq}$ and D.

From the interpolation maps (Fig. 8), it could be observed that the activities of the radionuclides varied from one location to another. This depicts that the activity concentrations of the radionuclides depended on the geological properties of soils and rocks along the coast of Ghana which differs with respect to the location. Both $^{226}$Ra and $^{232}$Th generally recorded low activities and were observed along the western parts of the coastline, whereas high concentrations were observed for the central and eastern parts. This could mean that $^{226}$Ra and $^{232}$Th correlated in their levels of abundance in the geographical areas. On the other hand, $^{40}$K and $^{137}$Cs showed uneven distribution patterns for the study area. In order to develop the awareness of the radiological hazard of beach sediment sampled from the study area, the spatial distribution map of the radiological hazards ($Ra_{eq}$ and D) along the coastline of Ghana showed that these parameters primarily depended on the $^{226}$Ra, $^{232}$Th and $^{40}$K activities for the individual locations and their interpolations were somehow similar to that of the radionuclides particularly $^{226}$Ra and $^{232}$Th.

## 4. Conclusions

In this study, the distribution of radionuclides emitting gamma radiation were studied in beach sediment samples collected along the coastline of Ghana. The mean activity concentrations of $^{226}$Ra, $^{232}$Th, $^{40}$K and $^{137}$Cs from the sampled coastal zones were determined. The results were compared with worldwide means, and they were found to be below the recommended values given by UNSCEAR except for $^{226}$Ra. The activities were also compared to the results of studies conducted in other countries and they were found to be similar except for the mean concentration of $^{137}$Cs. Radiological risk parameters such as $Ra_{eq}$, $H_{ex}$, $H_{in}$, D, $I_{\gamma}$, AED and AGDE were assessed to evaluate the impact of the radionuclides on human health. Their averages were calculated as 104.7 $Bqkg^{-1}$, 0.3, 0.4, 50.1 $nGyh^{-1}$, 0.4, 61.5 $\mu Svy^{-1}$ and 348.1 $\mu Svy^{-1}$, respectively. They were also below the worldwide reference levels, except for some areas which had high AGDE values. Due to the low $Ra_{eq}$, $H_{ex}$ and $H_{in}$ values, sediment from the study area could be used as building materials. However, high AGDE values recorded at some locations can pose radiation risks to the people. Multivariate statistical analysis was carried out on the measured radionuclides and radiological parameters determined. The results showed that only $^{226}$Ra and $^{232}$Th were normally distributed for the Kolmogorov-Smirnov test. A Person correlation analysis indicated that there is a strong

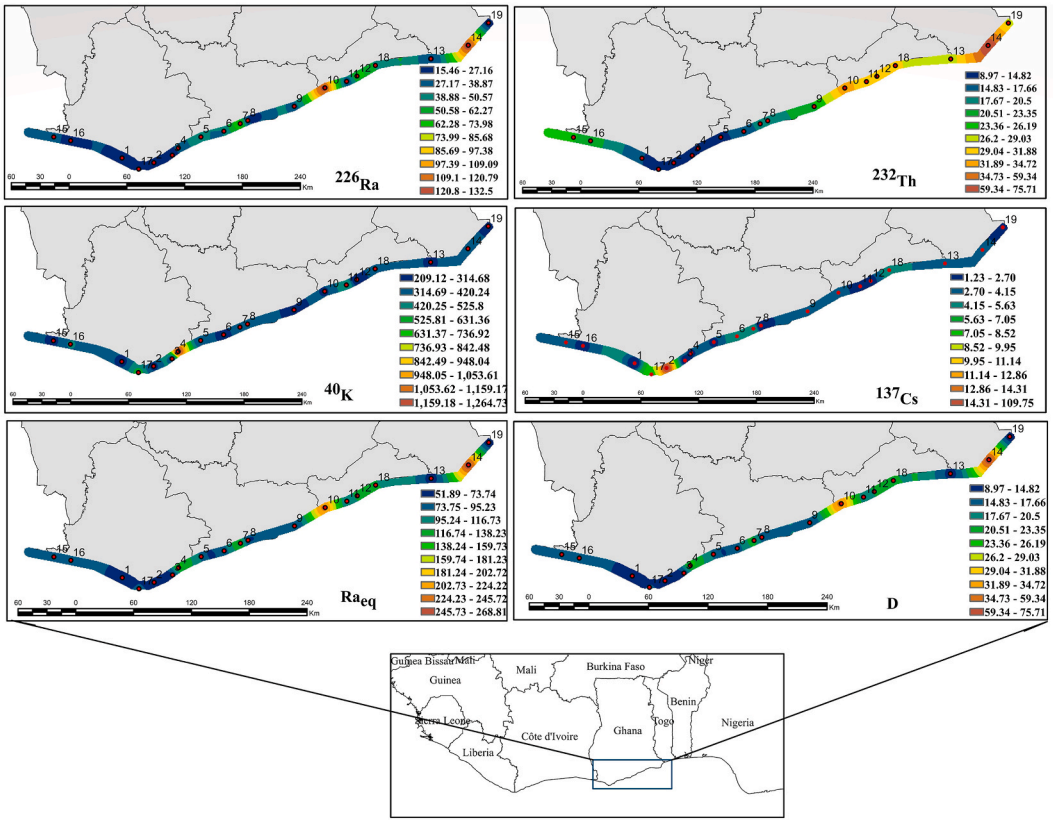


**Fig. 8.** Interpolation maps for the distribution of radionuclides and some radiological hazards ($^{226}$Ra, $^{232}$Th, $^{40}$K, $^{137}$Cs, $Ra_{eq}$ and D) along the coastline of Ghana.

relationship between the activities of $^{226}$Ra and $^{232}$Th. Similar observations were made from cluster and PCA analyses. Radiological maps were also generated for the study area to visualize the distribution of the measured radionuclides along the coast of Ghana. Apart from the high radionuclide activities recorded at few sample locations, it is generally assumed that sediments from Ghana's coast does not pose threat to the inhabitants of the area and the use of such sediments would not cause significant radiological health risk to the population. Nonetheless, it might increase over longer periods, particularly for the high concentration locations since comparison to previous studies showed a level of increment. A continuous monitoring of radionuclides along the shores of Ghana is however highly recommended, especially for the area which recorded high $^{137}$Cs activity. The results of this survey would form a reference data and could be regarded as baseline for future studies. It could also offer a level of baseline for recommending standards on natural and artificial radioactivity levels and its mapping for the coastline of Ghana. Nonetheless, there were a few drawbacks in this study, such as increasing the number of coastal zones sampled would have increased the number of samples collected for more data to be gathered on the distribution of radionuclides along Ghana's coast. However, time and resources were the constraints. Perhaps apart from gamma ray spectrometry, other spectrometric techniques such as alpha beta spectrometry and liquid scintillation counters could have also been used to measure the natural radionuclides in the sediments.

### *Author contribution statement*

Esther Osei Akuo-ko; Mohammademad Adelikhah: Conceived and designed the experiments; Performed the experiments; Analyzed and interpreted the data; Wrote the paper.

Eunice Amponsem; Anita Csordas: Analyzed and interpreted the data; Contributed reagents, materials, analysis tools or data.

Tibor Kovács: Conceived and designed the experiments; Analyzed and interpreted the data; Contributed reagents, materials, analysis tools or data; Wrote the paper.

## Data availability statement

Data included in article/supp. material/referenced in article.

## Declaration of competing interest

The authors declare that they have no known competing financial interests or personal relationships that could have appeared to influence the work reported in this paper.

## References

[1] M.H. Zakaly, M.A.M. Uosif, S.A.M. Issa, H.O. Tekin, H. Madkour, M. Tammam, A. El-Taher, G.A. Alharshan, M.Y.A. Mostafa, An extended assessment of natural radioactivity in the sediments of the mid-region of the Egyptian Red Sea coast Hesham, Mar. Pollut. Bull. 171 (2021), 112658.
[2] Y. Huang, X. Lu, X. Ding, T. Feng, Natural radioactivity level in beach sand along the coast of Xiamen Island, China, Mar. Pollut. Bull. 91 (2015) 357–361.
[3] H.K. Shuaibu, M.U. Khandaker, T. Alrefae, D.A. Bradley, Assessment of natural radioactivity and gamma-ray dose in monazite rich black Sand Beach of Penang Island, Malaysia, Mar. Pollut. Bull. 119 (2017) 423–428.
[4] M.O. Isinkaye, H.U. Emelue, Natural radioactivity measurements and evaluation of radiological hazards in sediment of Oguta Lake, South East Nigeria, J. Radiat. Res. Appl. Sci. 8 (2015) 459–469.
[5] B.O. Botwe, A. Schirone, I. Delbono, M. Barsanti, R. Delfanti, P. Kelderman, E. Nyarko, P.N.L. Lens, Radioactivity concentrations and their radiological significance in sediments of the Tema Harbour, Greater Accra, Ghana, J. Radiat. Res. Appl. Sci. 10 (2017) 63–71.
[6] ICRP, Lung Cancer Risk from Radon and Progeny and Statement on Radon, Annals of the ICRP, New York, NY, USA, 2010.
[7] M. Imani, M. Adelikhah, A. Shahrokhi, G. Azimpour, A. Yadollahi, E. Kocsis, E. Toth-Bodrogi, T. Kovács, Natural radioactivity and radiological risks of common building materials used in Semnan Province dwellings, Iran, Environ. Sci. Pollut. Control Ser. 28 (30) (2021) 41492–41503.
[8] A. Shahrokhi, M. Adelikhah, S. Chalupnik, T. Kovács, Multivariate statistical approach on distribution of natural and anthropogenic radionuclides and associated radiation indices along the north-western coastline of Aegean Sea, Greece, Mar. Pollut. Bull. 163 (2021), 112009.
[9] A. Amekudzie, G. Emi-Reynolds, A. Faanu, E.O. Darko, A.R. Awudu, O. Adukpo, L.A.N. Quaye, R. Kpordzro, B. Agyemang, B. Ibrahim, Natural radioactivity concentrations and dose assessment in shore sediments along the coast of Greater Accra, Ghana, World Appl. Sci. J. 13 (11) (2011) 2338–2343.
[10] M.A.E. Chaparro, G. Suresh, V. Ramasamy, M. Sundarrajan, Magnetic assessment and pollution status of beach sediments from Kerala coast (southwestern India), Mar. Pollut. Bull. 117 (2017) 171–177.
[11] E. Nyarko, B.O. Botwe, J.E. Ansong, R. Delfanti, M. Barsanti, A. Schirone, I. Delbono, Determination of $^{210}$Pb, $^{226}$Ra and $^{137}$Cs in beach sands along the coastline of Ghana, African J. Environ. Pollut. Health 9 (2) (2011) 17–23.
[12] S. Dizman, F.K. Görür, R. Keser, O. Görür, The assessment of radioactivity and radiological hazards in soils of Bolu province, Turkey, Environ. Forensics 20 (3) (2019) 211–218.
[13] S. Dizman, F.K. Görür, R. Keser, Determination of radioactivity levels of soil samples and the excess of lifetime cancer risk in Rize province, Turkey, Int. J. Radiation Res. 14 (3) (2016) 1–10.
[14] UNSCEAR, Sources of Ionizing Radiation. Volume 1. New York: United Nations Science Committee Effective Atomic Radiation, 2008.
[15] UNSCEAR, Sources, Effects and Risks of Ionizing Radiation: Report to the General Assembly with Annexes, United Nations Science Committee Effective Atomic Radiation, New York, 2000.
[16] L. Zhao, D. Liu, J. Wang, J. Du, X. Hou, Y. Jiang, Spatial and vertical distribution of radiocesium in seawater of the East China Sea, Mar. Pollut. Bull. 128 (2018) 361–368.
[17] G. Mouri, V. Golosov, M. Shiiba, T. Hori, Assessment of the caesium-137 flux adsorbed to suspended sediment in a reservoir in the contaminated Fukushima region in Japan, Environ. Pollut. 187 (2014) 31–41.
[18] A. Kitamura, M. Yamaguchi, H. Kurikami, M. Yui, Y. Onishi, Predicting sediment and cesium-137 discharge from catchments in eastern Fukushima, Anthropocene 5 (2014) 22–31.
[19] H. Foy, I. Bosman, Nuclear Energy in Ghana. Special Report. South African Institute of International Affairs (SAIIA), 2021, pp. 1–49.
[20] M.V. Ramana, P. Agyapong, Thinking big? Ghana, small reactors, and nuclear power, Energy Res. Social Sci. 21 (2016) 101–113.

[21] E.K. Quansah, Preliminary studies on impacts of ocean acidification on diversity of fish species landed by artisanal and semi-industrial fisheries and coastal community livelihoods in Ghana, in: Master's Thesis. University of Ghana, 2014, pp. 1–111.
[22] B.N. Alabi-Doku, S. Chen, E.H. Alhassan, Y. Abdullateef, M.M. Rahman, Fisheries resources of Ghana: present status and future direction, Int. J. Fisheries Aquatic Res. 3 (4) (2018) 35–41.
[23] A. Shahrokhi, M. Adelikhah, S. Chalupnik, E. Kocsis, E. Toth-Bodrogi, T. Kovács, Radioactivity of building materials in Mahallat, Iran–an area exposed to a high level of natural background radiation–attenuation of external radiation doses, Mater. Construcción 70 (340) (2020) e233.
[24] M. Adelikhah, A. Shahrokhi, M. Imani, S. Chalupnik, T. Kovács, Radiological assessment of indoor radon and thoron concentrations and indoor radon map of dwellings in Mashhad, Iran, Int. J. Environ. Res. Publ. Health 18 (1) (2021) 141.
[25] M. Adelikhah, A. Shahrokhi, S. Chalupnik, E. Tóth-Bodrogi, T. Kovács, High level of natural ionizing radiation at a thermal bath in Dehloran, Iran, Heliyon 6 (7) (2020), e04297.
[26] E. Kocsis, E. Tóth-Bodrogi, A. Peka, M. Adelikhah, T. Kovács, Radiological impact assessment of different building material additives, J. Radioanal. Nucl. Chem. 330 (3) (2021) 1517–1526.
[27] ICRP, ICRP Publication 60: 1990 Recommendations of the International Commission on Radiological Protection, 1991 no. 60). In: Elsevier Health Sciences.
[28] S.F. Özmen, A. Cesur, I. Boztosun, M. Yavuz, Distribution of natural and anthropogenic radionuclides in beach sand samples from Mediterranean Coast of Turkey, Radiat. Phys. Chem. 103 (2014) 37–44.
[29] B. Kucukomeroglu, A. Karadeniz, N. Damla, C.M. Yesilkanat, U. Cevik, Radiological maps in beach sands along some coastal regions of Turkey, Mar. Pollut. Bull. 112 (2016) 255–264.
[30] M.R. Abdi, S. Hassanzadeh, M. Kamali, H.R. Raji, $^{238}$U, $^{232}$Th, $^{40}$K and $^{137}$Cs activity concentrations along the southern coast of the Caspian Sea, Iran, Mar. Pollut. Bull. 58 (5) (2009) 658–662.
[31] A. Kubo, A. Tanabe, G. Suzuki, Y. Ito, T. Ishimaru, N. Kasamatsu-Takasawa, D. Tsumune, T. Mizuno, Y.W. Watanabe, H. Arakawa, J. Kanda, Radioactive cesium concentrations in coastal suspended matter after the Fukushima nuclear accident, Mar. Pollut. Bull. 131 (2018) 341–346.
[32] FAO/IAEA, Use of 137Cs for Soil Erosion Assessment. Fulajtar, 2017, pp. 1–64. E., Mabit, L., Renschler, C.S., Lee Zhi Yi, A., Food and Agriculture Organization of the United Nations, Rome, Italy.
[33] M. Yasumiishi, T. Nishimura, J. Aldstadt, S.J. Bennett, T. Bittner, Assessing the effect of topography on Cs-137 concentrations within forested soils due to the Fukushima Daiichi Nuclear Power Plant accident, Japan Earth Surface Dynamics 9 (2021) 861–893.
[34] T.-N. Nguyen, Q.-T. Tran, V.-P. Nguyen, N.-S. Le, S.-H. Phan, X.-T. Le, T.-T.-H. Vuong, V.-P. Nguyen, D.-T. Nguyen, D.-K. Tran, M.-D. Nguyen, Q.-T. Phan, T.-M.-T. Vo, V.-T. Duong, N.-C. Le, Activity concentrations of Sr-90 and Cs-137 in seawater and sediment in the gulf of tonkin, vietnam, J. Chem. (2020) 1–8.
[35] A.A. Abdel-Halim, I.H. Saleh, Radiological characterization of beach sediments along the Alexandria-Rosetta coasts of Egypt, J. Taibah Univ. Sci. 10 (2016) 212–220.
[36] S. Yamada, A. Kitamura, H. Kurikami, M. Yamaguchi, A. Malins, M. Machida, Sediment and 137Cs transport and accumulation in the ogaki dam of eastern Fukushima, Environ. Res. Lett. 10 (2015), 014013, 1-9.
[37] X. Liu, W. Lin, Natural radioactivity in the beach sand and soil along the coastline of Guangxi Province, China, Mar. Pollut. Bull. 135 (2018) 446–450.
[38] M. Sureshgandhi, R. Ravisankar, A. Rajalakshmi, S. Sivakumar, A. Chandrasekaran, D.P. Anand, Measurements of natural gamma radiation in beach sediments of north east coast of Tamilnadu, India by gamma ray spectrometry with multivariate statistical approach, J. Radiat. Res. Appl. Sci. 7 (2014) 7–17.
[39] K. Günoğlu, S. Seçkiner, Evaluation of dose parameters and radiological hazards in gravel samples of Konyaaltı Beach, Antalya, Arabian J. Geosci. 11 (16) (2018) 457.
[40] F. Otoo, E.O. Darko, M. Garavaglia, O.K. Adukpo, J.K. Amoako, J.B. Tandoh, S. Inkoom, S. Nunoo, S. Adu, Assessment of natural radioactivity and radon exhalation rate associated with rock properties used for construction in greater Accra region, Ghana, J. Radioanal. Nucl. Chem. 328 (2021) 911–923.
[41] F. Otoo, E.O. Darko, M. Garavaglia, C. Giovani, S. Pividore, A.B. Andam, J.K. Amoako, O.K. Adukpo, J.B. Tandoh, S. Inkoom, Public exposure to natural radioactivity and radon exhalation rate in construction materials used within Greater Accra Region of Ghana, Scientific African 1 (2018), e00009, 1- 12.
[42] C.E. Onwukwe, J.N. Ezeorah, Application of single-linkage clustering method in the analysis of growth rate of gross domestic product (GDP) at 1990 constant basic prices (million naira), Global J. Math. Sci. 8 (2) (2009) 83–93.